5

AuNP decorated PVA nanofiber as a SERS platform for trace detection of antibiotics in chicken meat

In this chapter, the exploration of AuNP decorated electrospun PVA nanofibers as a new SERS platform is presented. The surface morphological behavior of the fabricated SERS platform has been studied through FESEM characterizations, while TEM has been used to examine the synthesized nanoparticles. The fabricated SERS substrate has been used to detect trace concentration of two widely used poultry antibiotics - doxycycline hydrochloride (DCH), and enrofloxacin (ENX), in chicken meat samples. The validation of the presence of antibiotics in chicken meat samples has been accomplished using the standard analytical tool of liquid chromatography-mass spectrometry, and the results have been compared with the proposed sensing technique. Furthermore, PCA has been performed to classify the antibiotics present in the field-collected meat samples.

5.1 Introduction

The challenge of fabricating bio-compatible SERS substrate remains crucial while using them for infield sensing applications. Owing to the bio-compatible nature and excellent SERS base performance, several polymer-based SERS substrates have been explored in recent times. Out of there, is PVA standing out due to its easy and low-cost fabrication process. PVA is a polymer known for its hydrophilic, non-toxic properties and outstanding physical attributes such as thermal stability, strength, and water solubility [1]. Present chapter illustrates the functioning of AuNP-treated PVA nanofibers as a SERS substrate for trace sensing of antibiotics in chicken meat samples. Using the ex-situ synthesis protocol, the AuNP-treated nanofiber substrate has been fabricated by the electrospinning technique. The experimental procedure is depicted in figure 5.1.

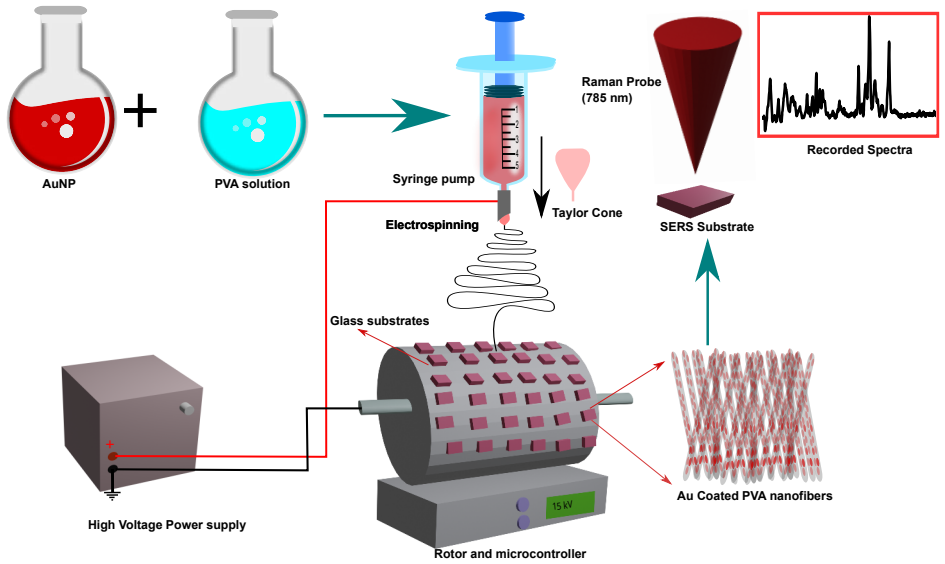

Figure 5.1: Schematic of the experimental setup

Previously, PVA electrospun nanofibers coated with AuNP, AgNPs and anisotropic metal nanostructures have been reported in various sensing applications, including environmental monitoring, food safety, biomedicine, explosive detection, and monitoring catalytic reactions [1]. The critical issue associated with anisotropic structures of electrospun fibers is their instability, potentially leading to SERS signal fluctuations over time. For this reason, spherical AuNPs have been considered in the present study to support the LSPR phenomenon. However, the major drawback of this sensing scheme is the large signal variations due to the non-uniform dispersion of nanoparticles over the SERS substrate. Additionally, depending on the applied voltage and concentration of the PVA solution, variations in the SERS signal may be observed. To address this issue, a study was conducted to optimize the SERS performance of the Au-PVA SERS substrate. A satisfactory SERS signal with a maximum signal variation of 5% was observed while maintaining an applied voltage of 15 kV and PVA concentration 8 wt% during the electrospinning process. With the incorporation of AuNPs in the PVA nanofibers, a significant improvement in the stability of the substrate has been observed [1]. The SERS signals from the samples remained stable over a period of 20 days. For both Raman active samples such as MG and R6G, the LoD for MG and R6G samples was found to be as low as 7.32 nM, surpassing earlier reported works [1]. With the proposed sensing technique, maximum signal variations of 5.57% and 5.65% were noticed for MG and R6G, respectively, thus indicating a good degree of reproducibility of the substrate. The usability of the designed substrate was realized through the detection of two commonly used poultry antibiotics, DCH and ENX. Upon observing reliable performance in the lab environment, the sensing scheme was extended for the trace sensing of these analytes in meat samples

acquired from the local meat market. For field collected samples ENX and DCH down to 0.3 ppm and 0.2 ppm, could be detected with the present sensing scheme.

5.2 Experimental

5.2.1 Chemicals

$HAuCl_4 \cdot 3\,H_2O$, $C_6H_5Na_3O_7 \cdot 2\,H_2O$, EDTA, acetonitrile, magnesium sulfate ($MgSO_4$), sodium chloride (NaCl) and PVA were purchased from Merck, India. MG and R6G were acquired from Alpha Aesar, India. DCH and ENX were obtained from a medical store. All the chemicals were used as received.

5.2.2 Synthesis of AuNPs

AuNPs has been synthesised in the laboratory using the conventional Turkevich method. In this synthesis procedure, auric chloride was reduced by sodium citrate. Briefly, 300 µL of 1 wt% $C_6H_5Na_3O_7 \cdot 2\,H_2O$ solution was added to 50 mL of boiling 0.01 wt% $HAuCl_4 \cdot 3\,H_2O$ under rapid stirring. After 15 min, the colour of the solution became dark red, indicating the formation of colloidal AuNP solution. The colloidal AuNP solution was then allowed to cool to room temperature. Figure 5.2(a) illustrates the TEM image of the synthesised AuNPs. From figure 5.2(b), the average diameter of the AuNPs has been estimated to be 28 nm.

5.2.3 Fabrication of SERS substrate

Figure 5.1 illustrates the schematic representation of the experimental setup employed in the present study. The unique characteristics of the Au-PVA substrate depend significantly on the alignment, size, shape, and spacing of electrospun PVA nanofibers on the glass substrate. Three different concentrations of PVA solutions (8 wt%, 10 wt%, and 12 wt%) were prepared in DI water at 80 °C under vigorous stirring. Subsequently, the synthesized AuNPs were blended with the PVA solutions, and the resulting PVA-AuNP solution was electrospun onto a microscopic glass slides measuring dimension of 1 cm × 1 cm. Prior to deposition, the glass slides were washed in ultrasonicated acetone bath, followed by rinsing with DI water and drying in a hot-air oven at 60 °C for 1 hour. The electrospinning system (ESPIN-NANO, India) was utilized for synthesizing the PVA nanofibers. Throughout the fabrication process, a constant flow rate (0.25 mLh^{-1}) was maintained. All glass slides were fixed on the rotor and the speed of the rotating drum was maintained at 1500 rpm. The separation distance between the syringe and the substrates was maintained at 15 cm. The deposited nanofibers were allowed to cross-linked at 180 °C for 1 hour

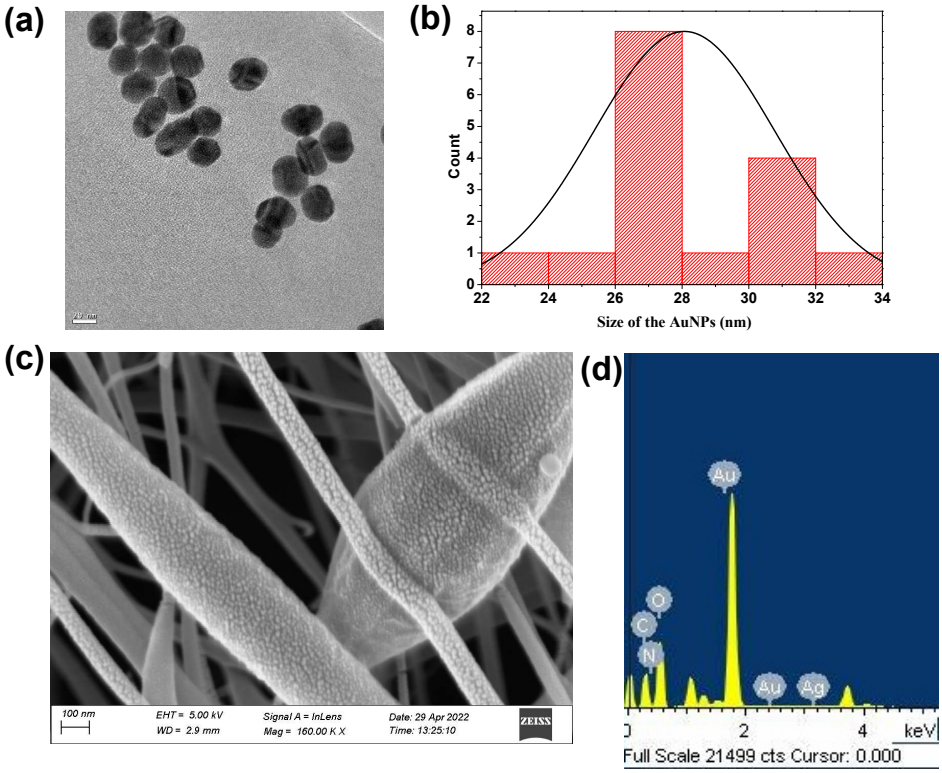

Figure 5.2: (a) TEM image of the synthesised AuNPs. Scale bar is 20 nm (b) histogram of the TEM image (c) FESEM image of the fabricated SERS substrate. Scale bar is 100 nm (d) EDX spectra of the SERS substrate indicating the element present

in a hot-air oven. Figure 5.2(c) presents the FESEM image of Au-PVA nanofibers, revealing variations in diameters ranging from 80 to 210 nm. Moreover, the spacing between nanofibers varied between 15 and 150 nm. Figure 5.2(d) displays the EDX data of the designed SERS substrate, indicating the presence of Au in the fabricated SERS substrate. Additionally, figure 5.3 shows the EDX elemental mapping of the designed SERS platform, demonstrating the uniform distribution of AuNPs across the fabricated SERS platform. The XPS analysis of the fabricated SERS platform has been performed and the results are shown in the figure 5.4. From the XPS analysis, the concentrations of Au, C and O are estimated to be 0.10%, 60.06% and 39.84% respectively. Figure 5.4(a) depicts the survey scan of the fabricated SERS substrate; the peaks near 87 eV, 283 eV and 531 eV confirm the presence of Au, C and O in the designed SERS substrate [5, 6]. Figure 5.4(b), (c) and (d) represent the high-resolution XPS spectra of Au 4f, C 1s and O 1s respectively. In figure 5.4(b), the two prominent peaks have been observed at 83.9 eV and 87.5 eV. These correspond to the Au $4f_{7/2}$ and Au $4f_{5/2}$ respectively, which confirms the presence of Au in the designed SERS substrate. In figure 5.4(c), the two peaks appearing at 285.8 eV and 286 eV confirm the presence of C 1s C−C and C 1s C−O of the fabricated SERS substrate. The single peak shown in figure 5.4(d) near 532.5 eV is attribute to O 1s

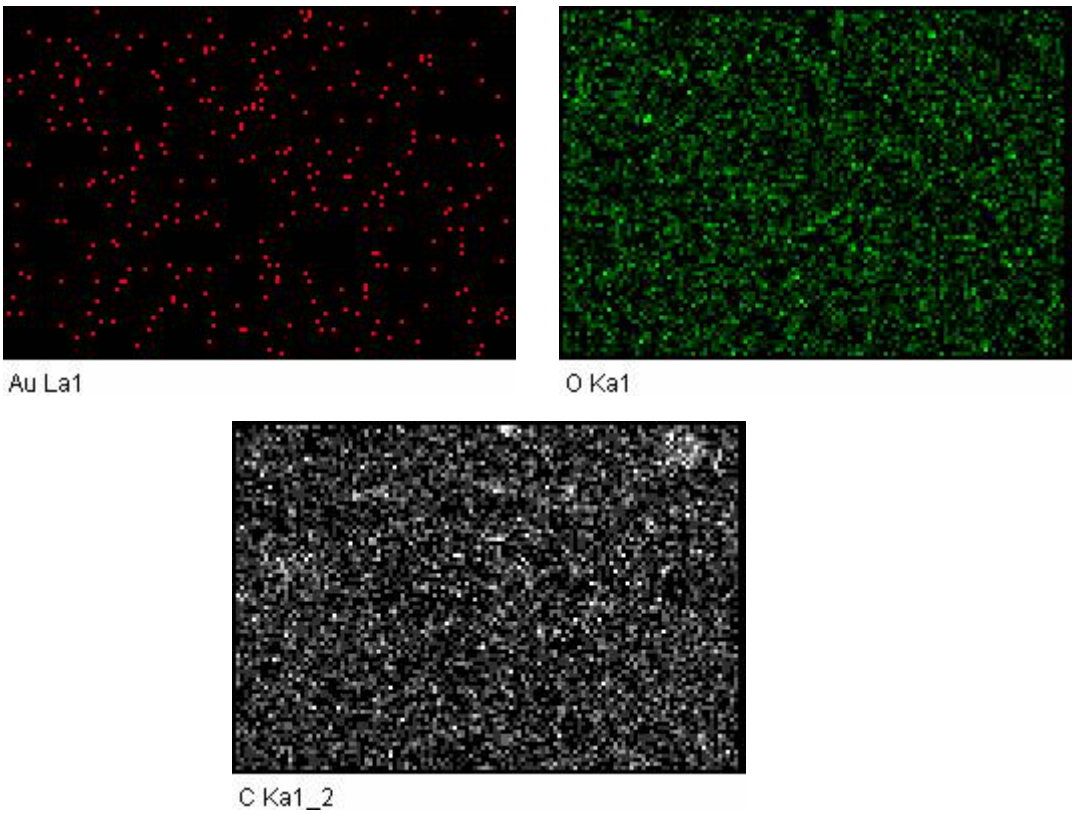

Figure 5.3: Elemental mapping of the SERS substrate indicating presence of gold, oxygen and carbon

state of the fabricated SERS substrate. These data reveal the presence of Au, C and O in the fabricated Au-PVA SERS substrate.

5.2.4 Meat samples

Meat samples were prepared according to the established protocol reported elsewhere [7]. In summary, approximately 500 grams of chicken liver, kidney, and muscle meats were individually homogenized in a laboratory blender. Four grams of grinded chicken meat from each part were weighed into a 20 mL centrifuge tube, followed by the addition of 4 mL of ultrapure water. The sample was then vortexed for 60 seconds and kept in a dark environment for 10 minutes. Subsequently, 1 mL of EDTA was introduced as a chelating agent. Ten milliliters of acetic acid (1%) in acetonitrile were added and vigorously shaken for 1 minute. This was followed by the sequential addition of 4 grams of $MgSO_4$ and 1 gram of NaCl to the solution. The resulting extract was centrifuged at 5000 rpm at 4 °C for 5 minutes and then allowed to settle for 30 minutes.

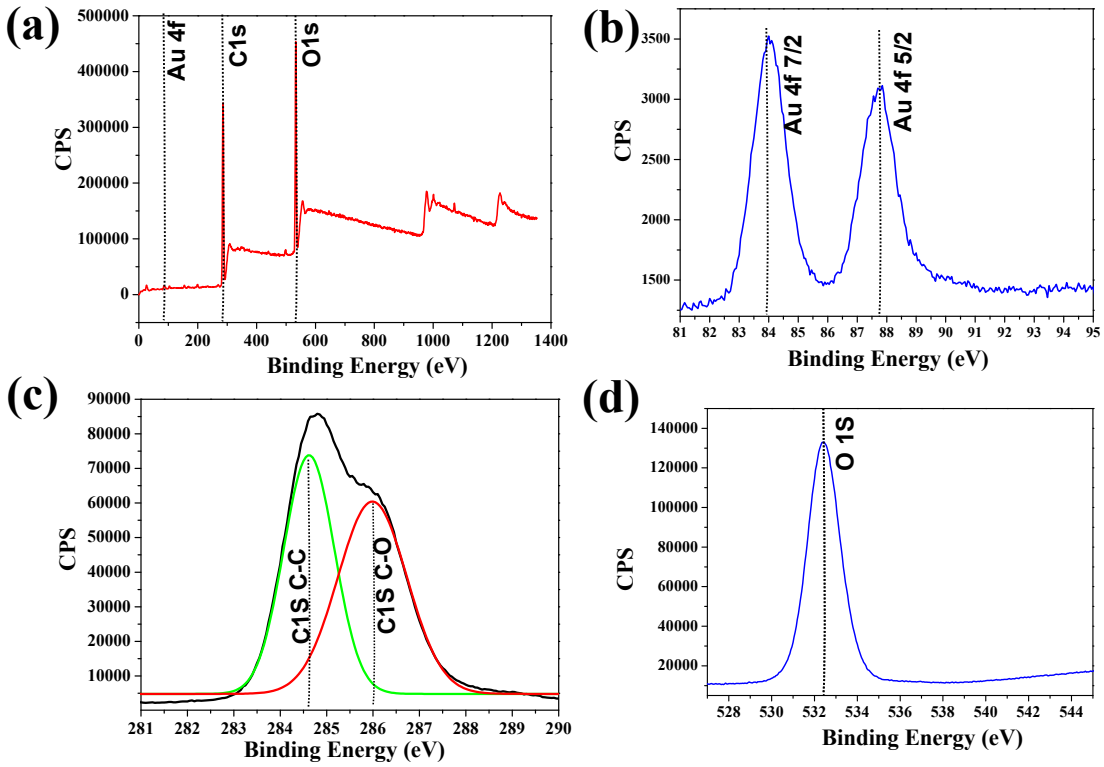

Figure 5.4: (a) XPS survey scan of the fabricated SERS substrate (b) High-resolution XPS spectra for (c) AuNP, (d) carbon, (e) oxygen

5.2.5 Raman instrumentation

The specification of the Raman instrumentation is described in the section 2.2.4.

5.2.6 Spectral acquisition

SERS spectra were obtained by pipetting 10 µL droplet of the analyte onto the fabricated Au-PVA SERS substrate. In the case of meat samples, 10 µL extract of the meat was deposited onto the sensing area and upon drying the analyte, the SERS spectra were recorded using the Raman spectrometer. The standard deviation was determined from five repetitions, and the error bars were incorporated in the plots. All spectra and calibration plots were generated using the same laser excitation wavelength of 785 nm.

5.2.7 EM simulation study of the LSPR field

EM simulation was performed for the considered SERS platform using COMSOL Multiphysics (version 5.2) software. In the present simulation study a linearly polarized laser source with a wavelength of 785 nm was used assumed at normal incidence on the Au-PVA SERS substrate. For estimating the coupled LSPR field amplitude, an average AuNP size of 30 nm and a nanofiber length of 150 nm has been assumed.

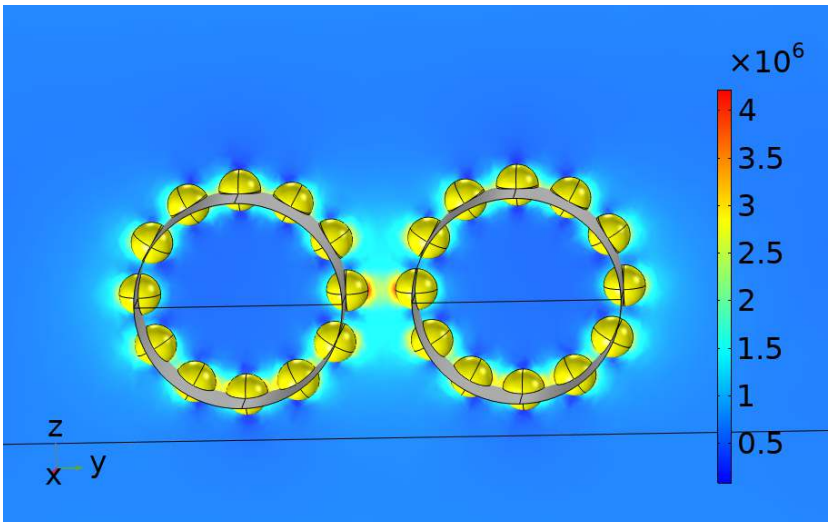

Figure 5.5: simulation of LSPR field magnitude for AuNPs distributed over PVA nanofibers; the incident electric field amplitude was assumed as $1.0 \times 10^5\,\mathrm{Vm}^{-1}$

The distribution of the EM field around the nanofibers is depicted in figure 5.5. A maximum field amplitude of $4.2 \times 10^6\,\mathrm{Vm}^{-1}$ has been observed for the designed SERS substrate. Additionally, another simulation was conducted to investigate the impact of the thickness of the fabricated nanofibers on the magnitude of the EM field, as illustrated in figure 5.6. It has been observed that the EM field amplitude decreased with increasing thickness of the nanofibers. In present simulation work the incident field amplitude was assumed as $1.0 \times 10^5\,\mathrm{Vm}^{-1}$. The details of EF, estimated through both simulation and experimental methods, are described in table 8.16.

5.2.8 Data analysis

PCA was used to analyse SERS spectral data using R data analysis software. Prior to the PCA analysis, spectral pre-treatments like binning, smoothing and normalisation of the spectral data were performed. In the present study, PCA was used to classify DCH and ENX in the meat samples of 26 different meat samples.

5.3 Results and discussion

5.3.1 Optimization of the SERS substrate

The performance of the fabricated SERS substrate has been evaluated across varying concentrations of PVA solutions and applied voltages during the nanofiber fabrication process. Figure 5.7(a) illustrates the relationship between SERS signal and the concentration of PVA solution, while figure 5.7(b) demonstrates the correlation between SERS signal and the applied voltage, with MG serving as test analyte. Amongst the

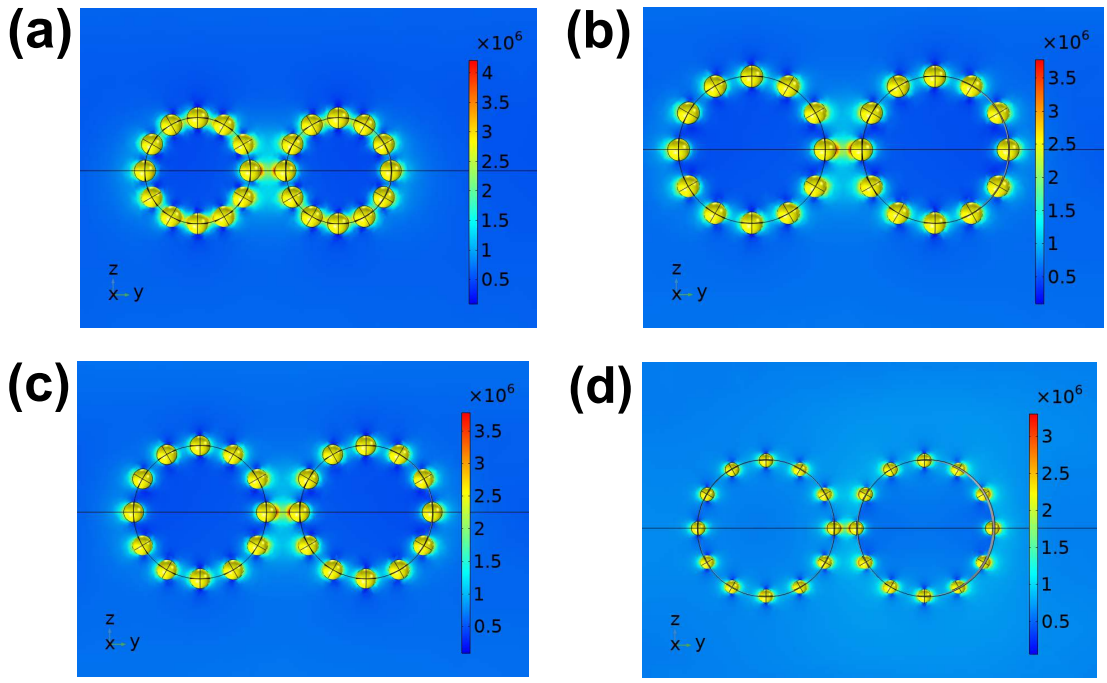

Figure 5.6: COMSOL Multiphysics simulation for the coupled EM field when the diameter of the nanofibers is (a) 150 nm (b) 200 nm (c) 250 nm (d) 300 nm; the incident electric field amplitude was assumed as $1.0 \times 10^5\,\mathrm{Vm}^{-1}$

different combinations of PVA concentrations and applied voltages, it has been found that nanofibers produced from 8 wt% PVA at an operational voltage of 15 kV yielded the best SERS performance in terms of signal enhancement factor and sensitivity.

5.3.2 Characterisation of the substrate

MG and R6G have been considered as the standard target analyte to evaluate the characteristic of the SERS substrate. Figure 5.8(a) illustrates the Raman signal intensity of MG scattered from the sensing region of the Au-PVA SERS substrate. The figure also includes backscattered signal of MG from glass, and on PVA nanofiber. Figure 5.8(b) and (c) present the SERS spectra of MG and R6G, respectively. SERS spectra of MG were examined at four different concentrations: 10 µM, 1 µM, 100 nM, and 10 nM. Similarly SERS spectra for R6G have been studied at four concentrations. It is evident that the characteristic Raman signal intensities of both samples gradually decrease with decreasing concentration of the analyte. Figure 5.8(d) and (e) illustrate the linearly fitted graphs of MG and R6G of ten different samples. The regression coefficient values for these two Raman-active samples were found to be R^2=0.98269 and R^2=0.94396, respectively. These values suggest a good degree of linearity of the proposed sensing scheme. For both MG and R6G, a linear relationship between SERS signal intensity and analyte concentration has been observed. With the proposed SERS platform sample concentrations as low as 10 nM for both standard samples

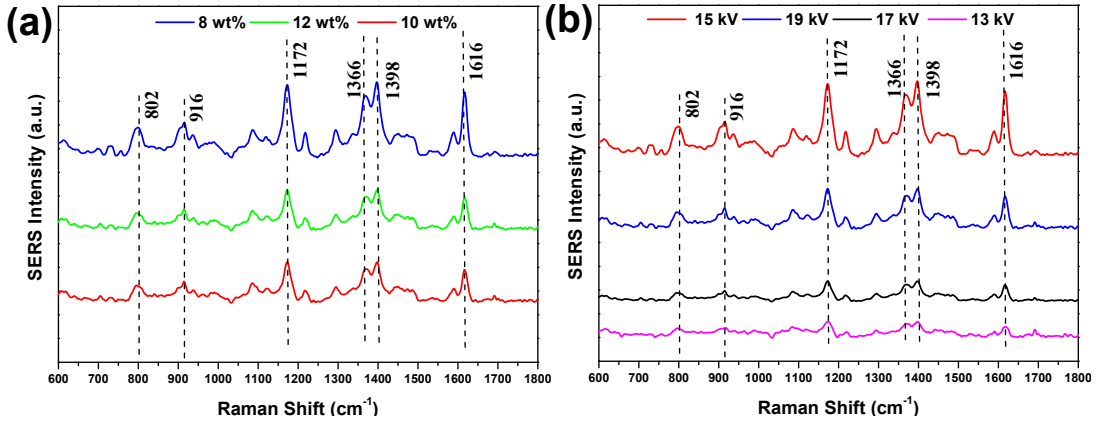

Figure 5.7: (a)Variation of SERS spectra of MG with different concentration of PVA solution in the fabrication procedure (b) Variation of SERS spectra of MG with applied voltage of the electrospinning setup

can be detected.

The Raman band assigment for MG and R6G have been illustrated in appedix (table 8.1 and table 8.2) [8, 9]

5.3.3 Reproducibility and uniformity characteristics

The reproducibility performance of the designed SERS substrate has been evaluated and the result is depicted in figure 5.9. MG of concentration 1 µM was initially drop-casted over ten identical SERS substrates. The scattered Raman signal intensity from the analytes were recorded from five random locations from each SERS substrate. Figures 5.9(a) and 5.9(b) illustrate the reproducibility characteristics of the proposed SERS substrate. The maximum RSD values were observed to be 5.31%, 5.13%, and 5.57% for the signature Raman peaks of MG at 1172 cm^{-1}, 1398 cm^{-1}, and 1618 cm^{-1}, respectively. For R6G, these values at 770 cm^{-1}, 1362 cm^{-1}, and 1510 cm^{-1} were found to be 5.39%, 5.21%, and 5.65%, respectively. These low RSD values suggest that the fabricated substrate is highly reproducible.

Additionally, to assess the spectral uniformity of the substrate, Raman mapping was conducted for MG focusing on the signature Raman peak at 1398 cm^{-1}. An array of 15 × 15 was considered over an area of 1 mm × 1 mm on the sensing area of the substrate. Figure 5.8(f) displays the variation in scattered Raman signal intensity corresponding to the wavenumber 1398 cm^{-1} of MG. A maximum variation of 10% was observed, suggesting that the proposed substrate possesses reasonably uniform characteristics when detecting scattered Raman signals of the sample.

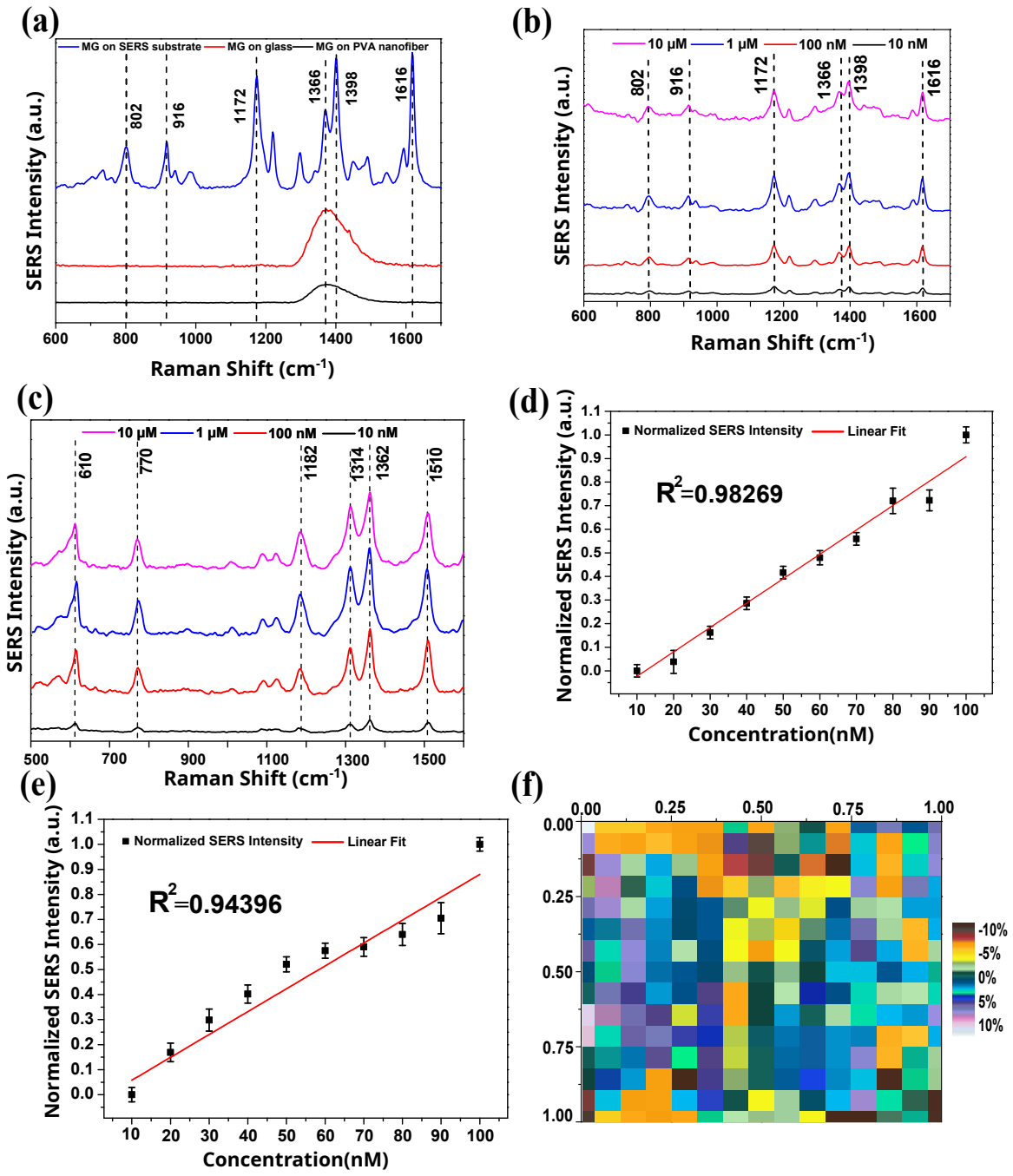

Figure 5.8: (a) Backscattered Raman signal intensity of MG recorded on Au-PVA SERS substrate, on glass and on PVA nanofiber (b) SERS spectra of MG at various concentrations (c) SERS spectra of R6G at various concentrations (d) Fluctuations of normalised SERS signal intensity with the change in concentrations for MG at signature Raman peak 1398 cm^{-1} (e) Fluctuations of normalised SERS signal intensity with the change in concentrations for R6G at signature Raman peak 1362 cm^{-1} recorded at 785 nm excitation for five repeated runs for each sample (f) SERS intensity variations mappings on 1 mm $\times$1 mm of the substrate when Raman peak at 1398 cm^{-1} of MG was considered as an analyte over a sensing area of the substrate; (Error bars are plotted using the standard deviation, calculated from five repetitions for each sample)

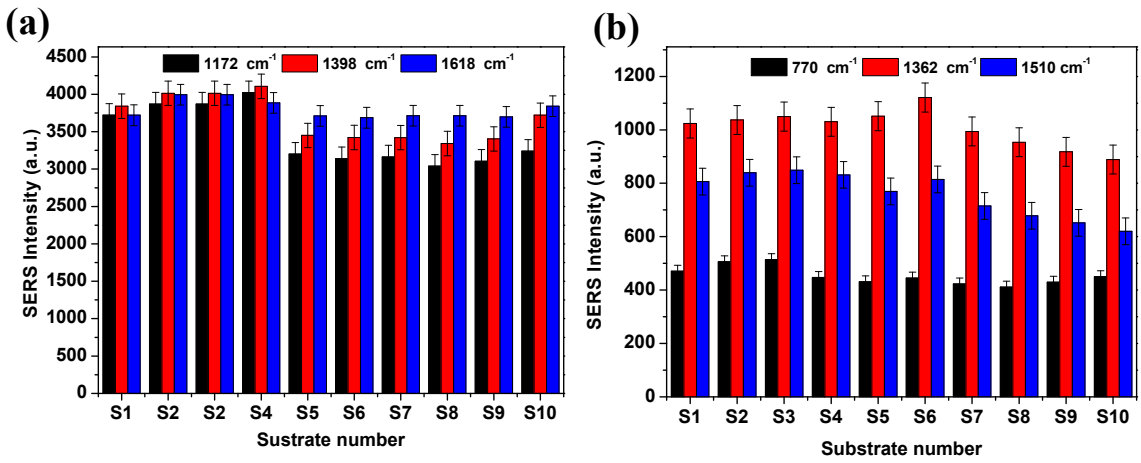

Figure 5.9: (a) Reproducibility characteristics of MG for ten different substrates with five repeitions for each sample (b) Reproducibility characteristics of R6G for ten different substrates with five repeitions for each sample; (Error bars are plotted using the standard deviation, calculated from five repetitions for each sample)

5.3.4 Temporal evaluation

To evaluate the stability of the fabricated SERS platform, a time stability analysis was performed. In this analysis, 1 µM of the test sample MG was applied to the sensing region of the SERS substrate, and the scattered Raman signals were recorded for a period of 24 days. Figure 5.10 illustrates the results of the time stability analysis. It is evident from figure 5.10 that the proposed sensing platform yields a fairly stable SERS signals over a period of 20 days.

5.3.5 Evalutation of EF

The EF of the designed substrate has been estimated following the procedure 2.3.4 and the values were estimated to be 1.31×10^6 and 1.51×10^6 for MG and R6G respectively.

5.3.6 Estimation of LoD

The LoD of the designed substrate has been determined using MG as a test analyte. Ten different concentrations of MG ranging from 10 nM to 100 nM were examined. The prepared samples were drop-casted onto various SERS substrates individually, and the Raman spectra were recorded. Figure 5.8(d) illustrates the relationship between normalized SERS intensity and concentration corresponding to the signature Raman peak at 1398 cm^{-1}. The LoD of the fabricated SERS substrate was calculated using equation 2.1 and was found to be 7.32 nM. A comparison among some of the previously reported works on nanofiber-based SERS substrate and the present SERS technique has been summarized in tabular form in the table 5.1.

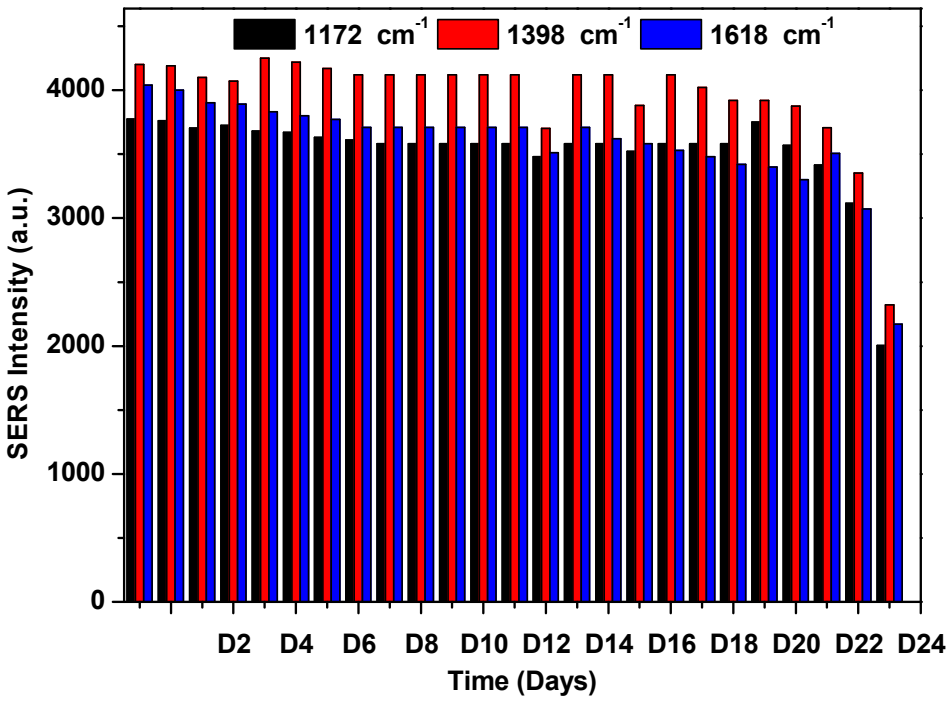

Figure 5.10: Time evaluation study of the fabricated SERS substrate taking MG as a test analyte recorded for 22 days

5.3.7 SERS analysis of DCH and ENX

In the final step of the experimental work, the practical utility of the present substrate has been demonstrated through detection of two commonly used poultry antibiotics, DCH and ENX. A stock solution of 10 ppm was prepared in DI water. Three additional concentrations (1 ppm, 0.5 ppm, and 0.2 ppm) of DCH and ENX were prepared by diluting the stock solution with an appropriate amount of DI water. All samples were treated with a fixed volume of 10 µL and dried under ambient room temperature conditions. Figure 5.11(a) displays the SERS spectra of DCH recorded from the Au-PVA SERS substrate. The DCH molecule contains several ketones (CO) and alcohol (OH) groups, along with the benzene ring, leading to the appearance of characteristic Raman peaks as depicted in figure 5.11(a).

The characteristic Raman peaks for DCH has been presented in appendix (see Table 8.11). Figure 5.11(c) displays the linearly fitted graphs with regression coefficient values of R^2=0.93685 for ten different DCH concentrations. Again, a linear correlation between SERS signal intensity and the variation in DCH concentration has been observed. By using the regression analysis, the concentration values can be calculated using equation 5.1.

$$Y = (-0.13929 \pm 0.05961) + (1.02323 \pm 0.08822)\, X \tag{5.1}$$

Figure 5.11(b) depicts the SERS spectra recorded from the ENX deposited SERS

Table 5.1: Comparison of the recently reported nanofiber-based SERS substrates

Material	Target Analyte	EF	RSD (%)	LoD(M)	Reference
Au/poly(vinylene fluoride), PLLA and nylon mats	E. coli, S. aureus, 4-MBA	10^6	22	Not specified	[10]
AuNPs on polyacrylonitrile 8-mercapto-9-propyladenine (L)	Uric acid	10^4	Not specified	10^{-7}	[11]
AgNP-decorated polyimide (PI) nanofabric	p-ATP	9.0×10^3	<20	10^{14}	[12]
NPs/PVA@Ag nanofibers	Sudan	6.04×10^8	12.89	10^8	[13]
AuNP-decorated PVA nanofibers	MG, R6G, DCH, ENX	10^7	10	7.32×10^9	This work

substrates. The attributes of Raman peaks for ENX has been provided in the appendix (see Table 8.12). Figure 5.11(d) illustrates the linearly fitted graphs with regression coefficient value $R^2 = 0.95137$ for ten different ENX concentrations. For ENX, concentration values can be calculated using the following calibration equation 5.2:

$$Y = (-0.05498 \pm 0.04574) + (1.05182 \pm 0.07905)\, X \tag{5.2}$$

5.3.8 SERS analysis of real samples

The applicability of the designed SERS substrate has been realised through sensing of poultry antibiotics in chicken meat samples. Chicken meat from a local poultry market has been obtained, and the sample extracts were prepared according to the protocol outlined in 5.2.4 section. Figure 5.12(a) displays the background spectra of the field-collected samples, while figure 5.12(b) illustrates the recorded Raman signal spectra of the meat samples.

The background Raman spectra originated from the presence of the solvent acetic acid in the meat extraction process. The peak assignments for the background sample are provided in table 8.13 of the appendix. The characteristic Raman peaks for DCH were observed at 883 cm^{-1} and 1141 cm^{-1}, while the other peaks of DCH appearing in the same figure are found to be altered for field-collected meat samples. For ENX, characteristic Raman peaks at 1253 cm^{-1}, 1395 cm^{-1}, 1465 cm^{-1}, 1536 cm^{-1}, and 1624 cm^{-1} were observed in the meat extract. Using calibration equations 5.1 and 5.2, the concentration of DCH and ENX present in the meat sample was estimated to be 0.238 ± 0.0024 ppm and 0.389 ± 0.0046 ppm, respectively, which exceeds the MRL prescribed by the EU ($\sim$ 0.1 ppm) [14]. From figure 5.12(b), it is evident

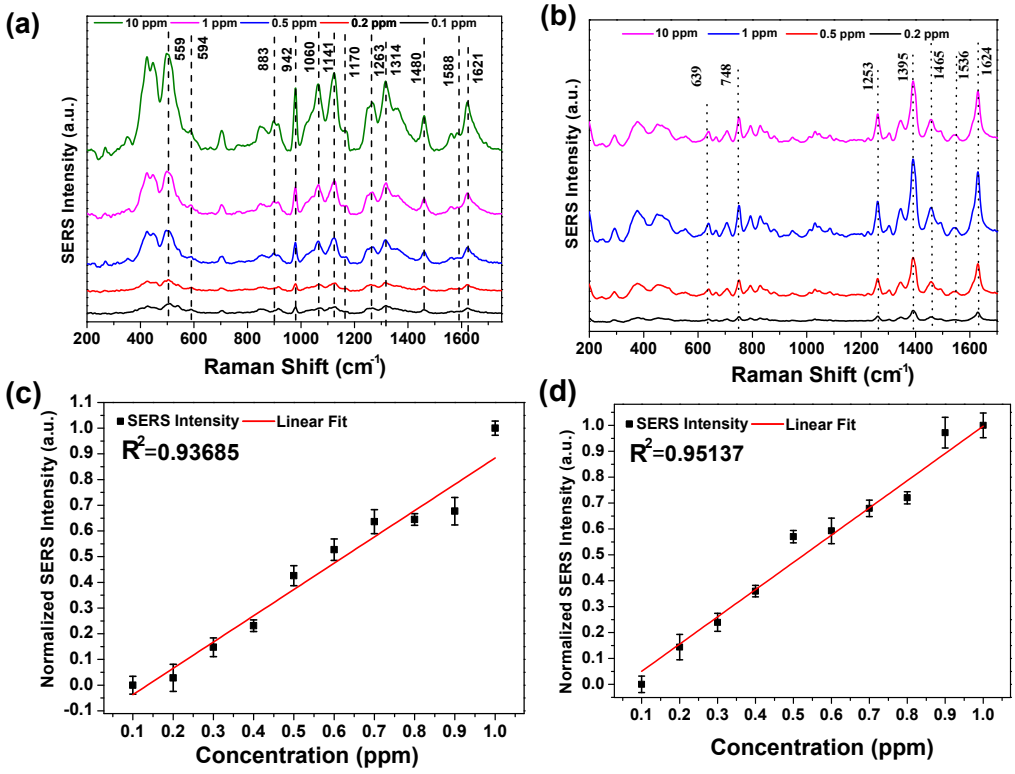

Figure 5.11: SERS spectra of (a) DCH and (b) ENX. For each sample, the spectra were recorded for five consecutive repetitions. Panels (c) and (d) represent the normalised SERS signal intensity corresponding to the Raman peak of DCH at 1141 cm^{-1} and ENX at 1395 cm^{-1} respectively; (Error bars are plotted using the standard deviation, calculated from five repetitions for each sample)

that the characteristic Raman peaks of the considered DCH and ENX can be reliably identified with the designed sensing platform. From figure 5.12(b), it is apparent that the considered antibiotics are more found more in qunatities in the livers compared to the other muscles and kidneys of chicken meat.

5.3.9 LC-MS of real samples

The presence of antibiotics in chicken meat samples was confirmed using LC-MS, a commonly employed method for such purposes. A good correlation has been observed between the experimental results obtained from the LC-MS data and the SERS-based sensing results proposed in this study. The chromatogram of the field-collected chicken meat sample is illustrated in figure 5.13. In figure 5.13, the peak at a retention time of 0.788 min corresponds to the analyte ENX; other peaks in the chromatogram appear from the solvent utilized in the extraction procedure [7].

Additionally, MS data corresponding to the chromatographic peak at 0.788 min is presented in figure 5.14. According to the LC-MS data, the MS peak at 361.2 $gmol^{-1}$ confirms the presence of ENX in chicken meat sample. However, MS peak for DCH couldn't be detected with the current LC-MS analysis method. This is attributed to the inefficiency of the sample extraction procedure [7]. Nevertheless, through SERS,

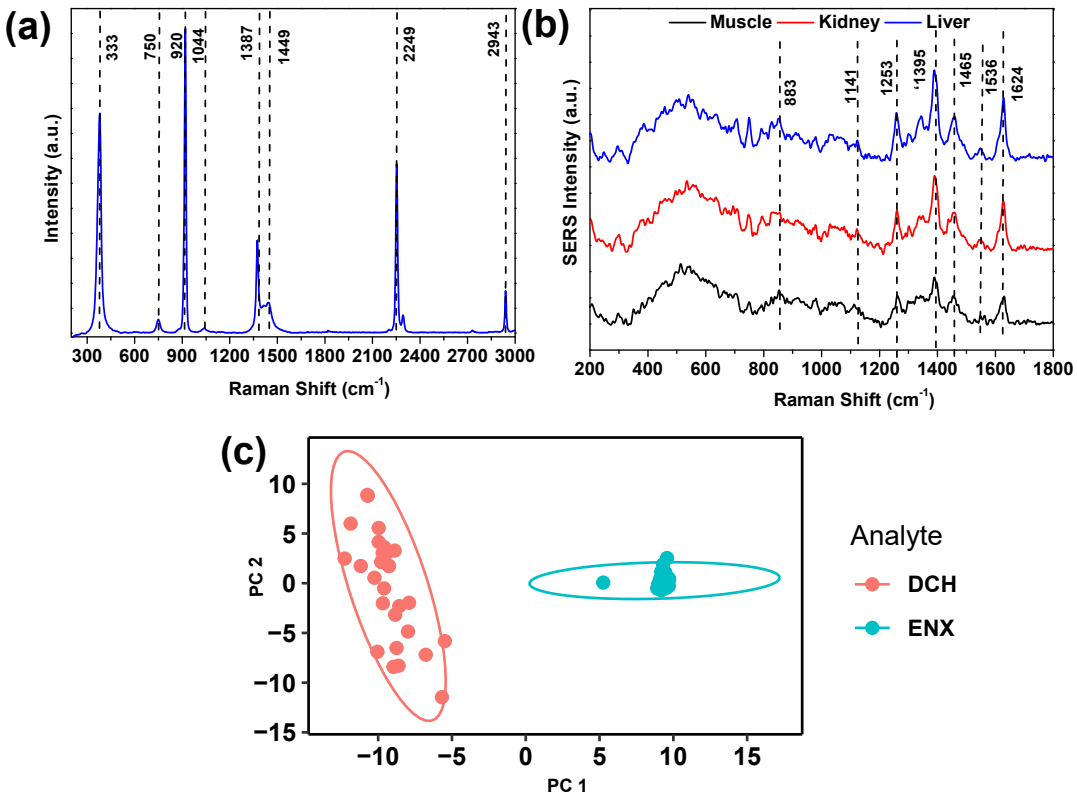

Figure 5.12: (a) Background spectra of the chemicals used in meat extract, (b) SERS spectra of field collected meat sample, (c) PCA score plot implemented to the field-collected meat samples

the characteristic Raman peaks of both DCH and ENX were clearly observed in the field-collected meat sample.

5.3.10 SERS analysis of spiked DCH and ENX in the meat Sample

In the next step of the present study, the field meat samples were spiked with the target analytes. A fixed concentration of 0.5 ppm of each sample has been spiked into the meat samples before the sample extraction. Upon spiking, the SERS analysis were performed. Figure 5.15 shows the recorded spectra for the spiked meat samples. Table 5.2 summarises the results obtained from the investigation. The low RSD values and high % recoveries for both the considered analytes again suggest the high reliability of the proposed sensing platform. The percentage recoveries have been calculated using the equation 5.3

$$\%recovery = \frac{Estimated\ conc}{Added\ conc} \times 100 \tag{5.3}$$

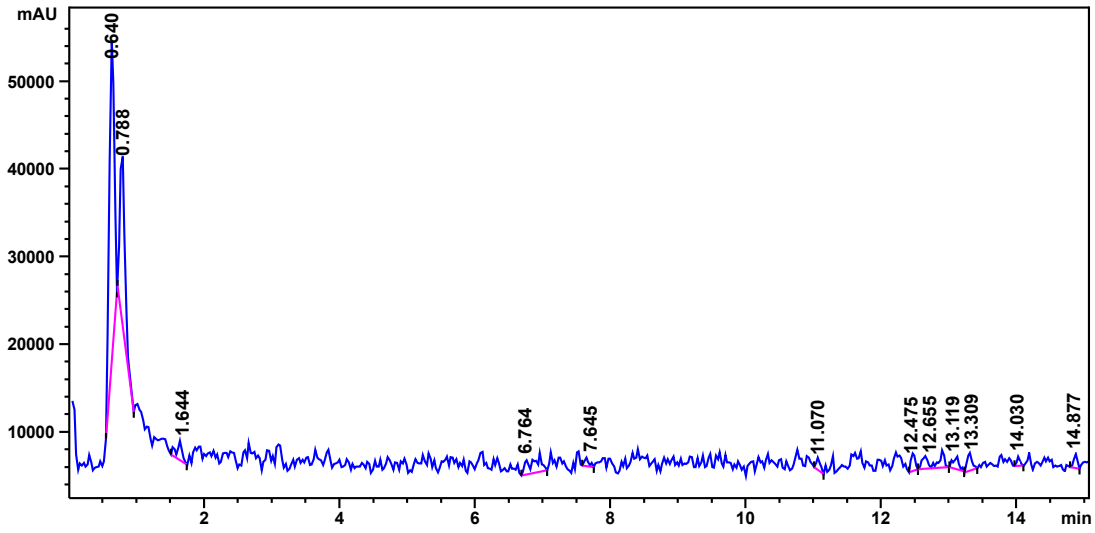

Figure 5.13: Chromatograph of the chicken meat sample

Table 5.2: SERS analysis of spiked DCH and ENX in the meat Sample

Analyte	Sample No	Added (ppm)	Estimated (ppm) (SERS)	Recovery (%)	RSD (%, n=5)	Estimated (LC-MS) (ppm)
DCH	S1	0.5	0.51	102	9.932%	Not detected
	S2		0.43	86		
	S3		0.51	102		
	S4		0.54	108		
	S5		0.44	88		
ENX	S1	0.5	0.42	84	13.418%	0.61
	S2		0.49	98		
	S3		0.61	122		
	S4		0.53	106		
	S5		0.51	102		

5.3.11 Implementation of multivariate analysis

In the final stage of the work, PCA analysis was performed to showcase the discriminating sensing capability for different analytes in the sample. Figure 5.12(c) illustrates the PCA score plot for the two analytes in the chicken meat sample. It is evident from figure 5.12(c) that DCH and ENX can be categorized within the mentioned principal components (PCs). The PCA analysis suggests that with the designed sensing platform, the target antibiotics can be detected and analyzed discriminately. This investigation further demonstrates that the proposed SERS-based sensing scheme is capable of identifying the mentioned antibiotics in meat samples in real-world conditions.

Despite the affordability of the proposed sensing method, it has two main drawbacks. Firstly, the deposition of electrospun nanofibers on a glass substrate is inherently random, leading to the inability to obtain highly ordered patterns of nanofibers. This would subsequently reduce the reproducibility characteristics over a wide sens-

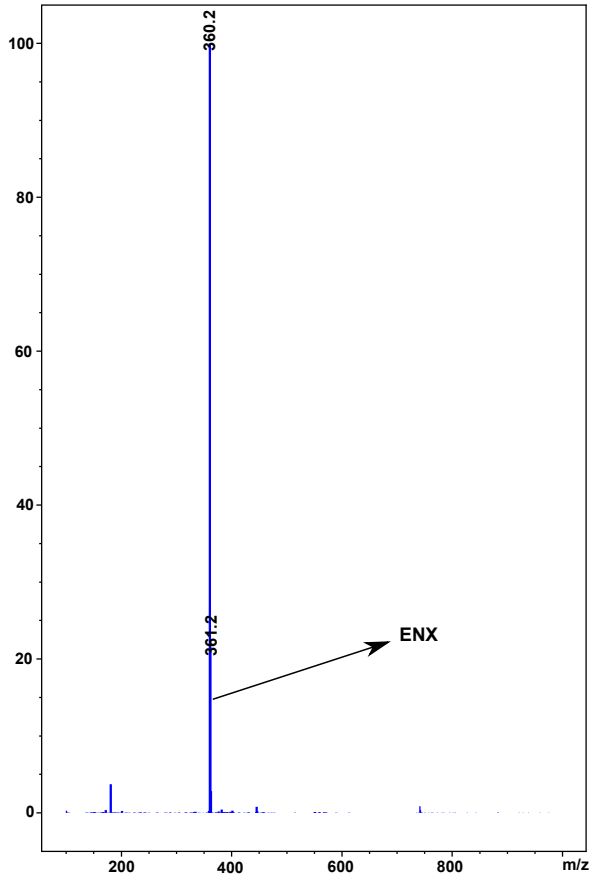

Figure 5.14: MS Data of the chicken meat sample

ing region of the SERS substrate. While the reproducibility of the SERS substrate has been evaluated over a sensing area of 1 mm × 1 mm, yielding a parameter as high as 90%, it drops to below 80% for a sensing area of 5 mm × 5 mm. Additionally, with the proposed fabrication procedure, generating SERS substrates with uniform surface morphology of nanofibers is challenging, even when the fabrication steps are repeated under identical conditions. This variations in surface morphology would lead to variations in the number of hotspot regions per unit area over the sensing region of the SERS substrate, causing fluctuations in the average Raman signal enhancement for different substrates.

5.4 Summary

The functioning of a cost-effective, sensitive, and acceptably reproducible SERS substrate is presented. By incorporating AuNPs into PVA electrospun nanofibers, the reliability of the designed SERS substrate for sensing of standard Raman-active dyes has been established. Upon notcing its reliable performance, the proposed scheme

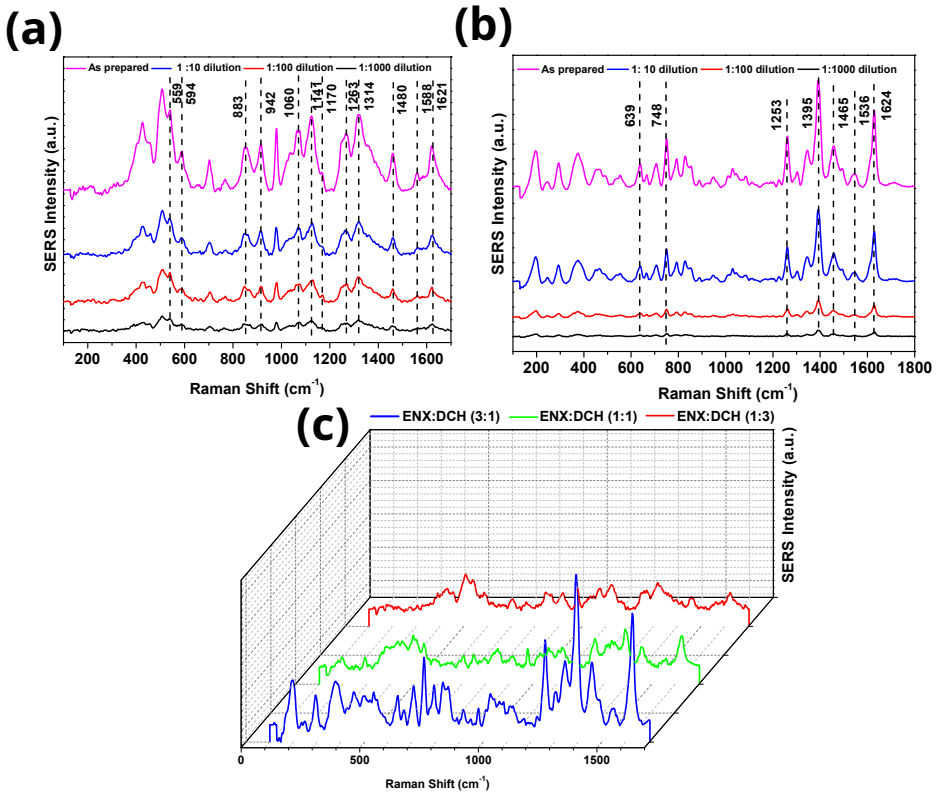

Figure 5.15: SERS spectra of the spiked meat sample with 0.5 ppm concentration

has been deployed to detect and quantify trace concentrations of two commonly used poultry antibiotics. Furthermore, the sensing scheme has been used to detect antibiotic drugs in field-collected meat samples. The PCA analysis of the spectral data revealed that the detection of the two antibiotics can be distinguished, indicating that this platform is reliable and suitable for detecting and analysing toxic chemicals present in the samples. It is anticipated that the proposed SERS scheme can serve as a rapid yet low-cost sensing platform for identifying antibiotics in animal husbandry. Detection of other drugs in various food matrices is also feasible with this sensing scheme and will be explored in future research endeavours.

References

[1] Pan, X., Bai, L., Pan, C., Liu, Z., and Ramakrishna, S. Design, Fabrication and Applications of Electrospun Nanofiber-Based Surface-Enhanced Raman Spectroscopy Substrate. *Critical Reviews in Analytical Chemistry*, pages 1–20, 2021. Publisher: Taylor & Francis.

[2] Wang, T., Liu, M., Huang, S., Yuan, H., Zhao, J., and Chen, J. Surface-enhanced Raman spectroscopy method for classification of doxycycline hydrochloride and

tylosin in duck meat using gold nanoparticles. *Poultry Science*, 100(6):101165, 2021.

[3] Xu, Y., Du, Y., Li, Q., Wang, X., Pan, Y., Zhang, H., Wu, T., and Hu, H. Ultrasensitive detection of enrofloxacin in chicken muscles by surface-enhanced raman spectroscopy using amino-modified glycidyl methacrylate-ethylene dimethacrylate (GMA-EDMA) powdered porous material. *Food analytical methods*, 7:1219–1228, 2014.

[4] Chen, Y., Cao, J., Wei, H., Wu, Z., Wei, Y., Wang, X., and Pei, Y. Fabrication of Ag NPs decorated on electrospun PVA/PEI nanofibers as SERS substrate for detection of enrofloxacin. *Journal of Food Measurement and Characterization*, 16(3):2314–2322, 2022.

[5] Alder, R., Hong, J., Chow, E., Fang, J., Isa, F., Ashford, B., Comte, C., Bendavid, A., Xiao, L., Ostrikov, K., et al. Application of plasma-printed paper-based SERS substrate for cocaine detection. *Sensors*, 21(3):810, 2021.

[6] Hashmi, M., Ullah, S., and Kim, I. S. Electrospun Momordica charantia incorporated polyvinyl alcohol (PVA) nanofibers for antibacterial applications. *Materials Today Communications*, 24:101161, 2020. Publisher: Elsevier.

[7] Jammoul, A. and El Darra, N. Evaluation of antibiotics residues in chicken meat samples in Lebanon. *Antibiotics*, 8(2):69, 2019. Number: 2 Publisher: MDPI.

[8] Bao, Z. Y., Liu, X., Chen, Y., Wu, Y., Chan, H. L. W., Dai, J., and Lei, D. Y. Quantitative SERS detection of low-concentration aromatic polychlorinated biphenyl-77 and 2, 4, 6-trinitrotoluene. *Journal of hazardous materials*, 280:706–712, 2014.

[9] Choi, C. J., Xu, Z., Wu, H.-Y., Liu, G. L., and Cunningham, B. T. Surface-enhanced Raman nanodomes. *Nanotechnology*, 21(41):415301, 2010. Number: 41 Publisher: IOP Publishing.

[10] Szymborski, T., Witkowska, E., Adamkiewicz, W., Waluk, J., and Kamiska, A. Electrospun polymer mat as a SERS platform for the immobilization and detection of bacteria from fluids. *Analyst*, 139(20):5061–5064, 2014. Number: 20 Publisher: The Royal Society of Chemistry.

[11] Saravanan, R. K., Naqvi, T. K., Patil, S., Dwivedi, P. K., and Verma, S. Purine-blended nanofiber woven flexible nanomats for SERS-based analyte detection. *Chemical Communications*, 56(43):5795–5798, 2020. Number: 43 Publisher: Royal Society of Chemistry.

[12] Kong, L., Dong, N., Tian, G., Qi, S., and Wu, D. Highly enhanced Raman scattering with good reproducibility observed on a flexible PI nanofabric substrate decorated by silver nanoparticles with controlled size. *Applied Surface Science*, 511:145443, 2020. Publisher: Elsevier.

[13] Zhao, X., Li, C., Li, Z., Yu, J., Pan, J., Si, H., Yang, C., Jiang, S., Zhang, C., and Man, B. In-situ electrospun aligned and maize-like AgNPs/PVA@ Ag nanofibers for surface-enhanced Raman scattering on arbitrary surface. *Nanophotonics*, 8 (10):1719–1729, 2019. Number: 10 Publisher: De Gruyter.

[14] Li, H., Wang, M., Shen, X., Liu, S., Wang, Y., Li, Y., Wang, Q., and Che, G. Rapid and sensitive detection of enrofloxacin hydrochloride based on surface enhanced Raman scattering-active flexible membrane assemblies of Ag nanoparticles. *Journal of environmental management*, 249:109387, 2019.